THE MIDDECK ACTIVE CONTROL EXPERIMENT (MACE)

David W. Miller[1], Raymond B. Sepe[2], Daniel Rey[3], Erik Saarmaa[4], Edward F. Crawley[5]
Space Engineering Research Center
Massachusetts Institute of Technology
Cambridge, Massachusetts

ABSTRACT

The Middeck Active Control Experiment (MACE) is a NASA In-Step and Control Structure Interaction (CSI) Office funded Shuttle middeck experiment. The objective is to investigate the extent to which closed-loop behavior of flexible spacecraft in zero gravity (0-g) can be predicted. This prediction becomes particularly difficult when dynamic behavior during ground testing exhibits extensive suspension and direct gravity coupling. On-orbit system identification and control reconfiguration is investigated to improve performance which would otherwise be limited due to errors in prediction. The program is presently in its preliminary design phase with launch expected in the summer of 1994.

The MACE test article consists of three attitude control torque wheels, a two axis gimballing payload, inertial sensors and a flexible support structure. With the acquisition of a second payload, this will represent a multiple payload platform with significant structural flexibility. This paper presents on-going work in the areas of modelling and control of the MACE test article in the zero and one-gravity environments. Finite element models, which include suspension and gravity effects, and measurement models, derived from experimental data, are used as the basis for Linear Quadratic Gaussian controller designs. Finite element based controllers are analytically used to study the differences in closed-loop performance as the test article transitions between the 0-g and 1-g environments. Measurement based controllers are experimentally applied to the MACE test article in the 1-g environment and achieve over an order of magnitude improvement in payload pointing accuracy when disturbed by a broadband torque disturbance. The various aspects of the flight portion of the experiment are also discussed.

INTRODUCTION

Objective and Rationale

The objective of the Middeck Active Control Experiment (MACE) is to develop a qualification procedure for flexible, precision spacecraft. For future vehicles which cannot be dynamically tested on the ground in a sufficiently realistic zero-gravity simulation, this procedure will increase confidence in the eventual orbital performance of such spacecraft (refs. 1 and 2). Confidence is developed through analysis and extensive ground testing. Analytical models, such as finite elements, require extensive refinement in order to achieve the accuracy required of high authority control (ref. 3). This refinement is enabled by modal identification (ref. 4). If suspension and gravity effects couple with the flexible behavior during ground testing, the analytical model must include these effects to ensure that the model is properly refined. However, the model will no longer accurately represent 0-g behavior.

An alternative to analytical models for control design is the development of measurement models (refs. 5 and 6). Transfer functions measured through the control hardware are fitted using an assortment of poles, zeros, gains and time delays. These models can provide high accuracy. However, if suspension and gravity effects are present in the measurements, the resulting control will be inappropriate for 0-g operation.

Therefore, the MACE program attempts to determine how a spacecraft designer might acquire confidence in the eventual on-orbit performance of a flexible spacecraft when the analytical 0-g predictions are inaccurate and the 1-g measurement models are inappropriate. To achieve this, the program follows the evolution of a 'CSI spacecraft' from analysis and ground testing through on-orbit system identification and control on board the middeck of the Shuttle. The test article is designed to couple suspension and direct gravity effects with the flexible behavior during ground testing (refs. 7 and 8).

[1] Principal Research Scientist, Member AIAA, ASME
[2] Postdoctoral Associate, Member IEEE
[3] Research Assistant
[4] Project Engineer
[5] Professor, Aeronautics and Astronautics, Member AIAA, ASME

Development Model Hardware Description

The Development Model (DM) is the first of three sets of hardware to be developed under the MACE program. As shown in Figure 1, the DM is composed of a three-axis torque wheel assembly, a two-axis gimballing payload, and a dummy mass which will be replaced by a second gimbal in the near future. When these components are connected by a flexible structural bus, the fundamental bending mode is 1.7 Hz.

The DM is instrumented with two angle encoders on the gimbal axes, two three axis rate gyro platforms, and other assorted sensors. One rate gyro platform is mounted in the payload while the other is mounted under the torque wheel assembly. The bus is composed of flexible Lexan™ struts interconnected by aluminum nodes. The torque wheel assembly is comprised of three orthogonally mounted DC servo motors with an aluminum inertia wheel mounted to each. Two-axis gimbal rotation is excited about the x and z axes via two DC torque motors.

The hardware components that serve as support equipment for the test article are a pneumatic/electric low-frequency suspension system (ref. 9), a real-time control computer (ref. 10), a Fourier analyzer, and various signal conditioning and power amplification electronics for the sensors and actuators, respectively.

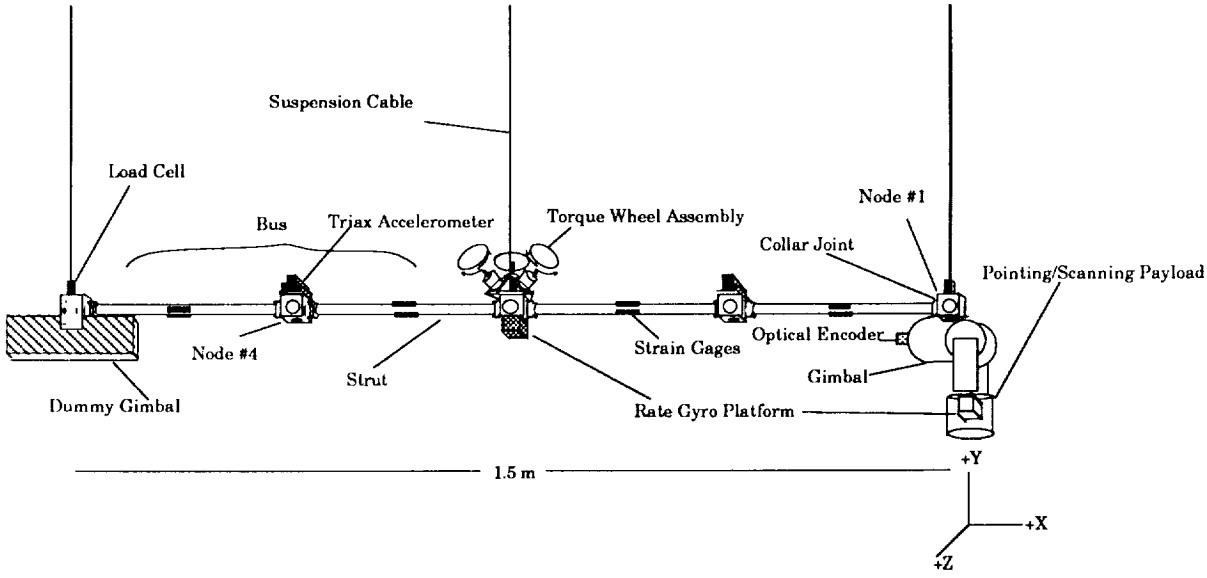

Figure 1. Development Model test article.

Science Approach

In the 1-g and 0-g control design for MACE, analytical finite element and measurement models are used in concert. This paper presents current progress along both avenues. Analytical models are useful in that they enable design work to be conducted prior to the acquisition of data or, for that matter, the test article itself. They also provide the crucial ability to predict on-orbit performance of flexible spacecraft. On the other hand, measurement models provide high accuracy and are essential for the design of high performance control.

Figure 2 illustrates how analytical model and measurement based control will be used in the MACE program to predict and develop high performance 0-g control. The figure represents open-loop identification and closed-loop control in two arenas: ground (1-g) and on orbit (0-g). The approach starts with the formulation of a 1-g finite element model. This model includes direct gravity and suspension effects in addition to the inertia, dissipation and elastic properties of the structure. The purpose of this model is to achieve as accurate a representation of 1-g behavior as possible. Finite element model accuracy is achieved through modal identification to correlate open-loop behavior and 1-g control implementation, and to identify critical dynamics which have been poorly modeled. By observing the degree to which this model is useful in the design of 1-g control, a sense for the limitations of 0-g predictions is obtained.

In parallel with the finite element modelling, measurement models are developed by fitting poles, zeros, gains and time delays to pertinent transfer functions through the control hardware. These models are used to derive control and can be refined based upon closed-loop results. Measurement models will generally provide higher accuracy than finite element models when low noise devices are used. Therefore, the closed-loop results reveal the practical limitations in performance improvement that can be obtained given a particular form of control formulation and architecture. By comparing this performance with that achieved using finite element based control, the designer can understand the cost-benefit of further finite element model refinement.

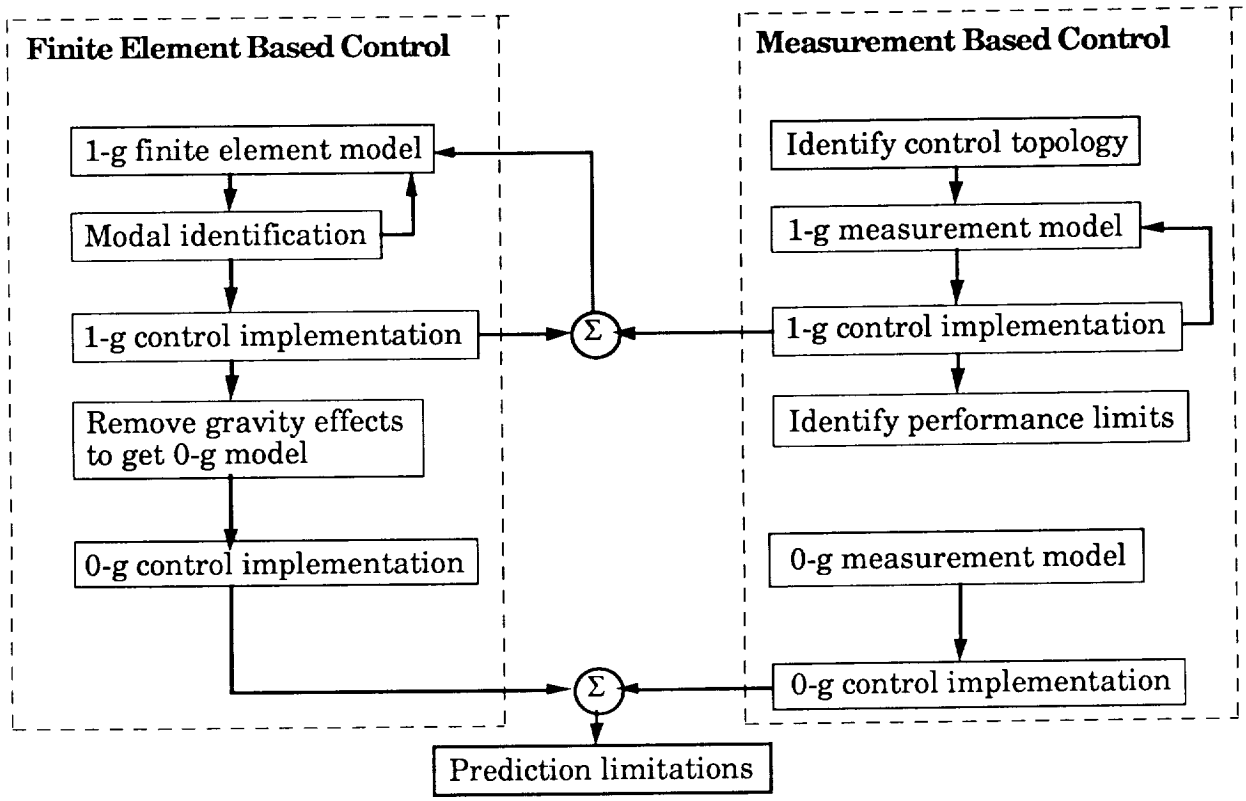

Figure 2. Science approach.

Once the finite element model has been sufficiently refined based upon ground testing, the gravity and suspension effects can be removed to yield a 0-g model. This model is then used to derive control for implementation on orbit. The accuracy of the 0-g finite element model can be assessed in open-loop by comparing predicted dynamics with 0-g system identification measurements acquired on orbit. It can also be assessed in closed-loop by comparing performance with both finite element predictions and 0-g measurement based control.

This science approach implies that on-orbit science operations will involve three phases. In the first phase, system identification will be performed to obtain measurement data for judging finite element model accuracy and deriving a 0-g measurement model. The second phase will involve the implementation of control algorithms based on the 0-g finite element model. During the third phase, control algorithms derived using the 0-g measurement model, developed using the system identification data, will be implemented.

This paper details some preliminary open and closed-loop results that have been obtained through analysis and ground testing. The next section develops both the 1-g and 0-g finite element models and analyzes the implications of testing the MACE test article in a 1-g environment when the control has been derived using a model of 0-g behavior. Such a scenario would be typical of preflight qualification testing for a flexible spacecraft. The following section discusses the use of 1-g measurement models to derive and exercise real time Linear Quadratic Gaussian (ref. 11) control on the MACE test article. This is followed by a brief description of the flight portion of the MACE program.

Suspension and Direct Gravity Effects

Ground-based test articles for research and qualification of precision spacecraft must be suspended in an effort to simulate the free-free boundary conditions of their operational environment. Under these conditions it is possible to group the perturbation effects of gravity on the dynamics of the controlled structure into five classes:

1) Suspension effects: The suspension system establishes the boundary conditions which affect the test article dynamics. All of the test article rigid-body modes are stiffened and the flexible modes couple to varying degrees with the suspension system dynamics.

2) Non-linear effects: This category encompasses all changes to the structural behavior due to gravity loading which must be modelled in a nonlinear fashion; e.g. loading of joints that have a deadband, gravity induced friction in articulations and devices, etc.

3) Stiffness Effects: The constant initial stress of the suspended structure due to gravity loading has the net effect of altering the structure's stiffness. This effect is a perturbation to the linear system model but can only be determined by taking into account the second order or quadratic strain terms in the equilibrium principle. Captured are the gravity stiffening and destiffening of the structural and suspension modes.

4) Static Pre-deformations: Given discrete suspension attach point locations, gravity loading will deform the structure and change the reference equilibrium about which the system dynamics are defined. Even slight deformations can couple otherwise decoupled modes.

5) Direct Sensor and Actuator Effects: The behavior of accelerometers and proof-mass actuators is directly affected by gravity when they are subject to harmonic orientation changes in a gravity field (ref. 12). The perturbation is additive and can result in amplifications, attenuations and even phase reversals of the device input or output.

The specific objective of the Middeck 0-gravity Dynamics Experiment (MODE) (ref. 13) was the study of the first two gravity influences with a particular focus on the non-linear gravity effects given the presence of a scaled space station alpha joint, tensioning cables which can slacken and numerous deployment hinges. MACE, the successor to the MODE experiment, is designed to investigate the first, third and fourth types of gravity effects on the dynamics of a flexible articulating multi-body test article in both open and closed-loop configurations.

Gravity Effect Modelling Procedure

The first step in including gravity effects into a finite element model of the MACE test article is the incorporation of the suspension system. Once this step is accomplished it is then possible to introduce the mass proportional gravity loading on the entire system and determine not only the static pre-deformations but also the gravity stiffening effects. This latter computation is the key to properly describing the system behavior in a gravity field.

Given a known internal stress state, it is possible to solve for a geometric or differential stress stiffness matrix which is a linear function of the loading. The static deformations are proportional to the loading and inversely proportional to the system stiffness matrix. However, the system stiffness matrix is itself a function of the loading and the system deformations. Therefore, it is necessary to iterate to solve for the static deformations.

The ADINA (Automatic Dynamic Incremental Nonlinear Analysis) (ref. 14) finite element modelling package was used to model both the MODE (ref. 15) and MACE test articles and as a research tool in the study of sample problems for the identification of gravity and suspension effects. Modelling gravity effects in ADINA is a multi-step procedure. If suspension system bounce frequency tuning is required to achieve mass proportional stiffnesses in the suspension devices, as was the case with the MACE pneumatic/electric suspension devices, it is necessary to initially perform a static reaction force analysis with the structure pinned at the attachment points. The suspension spring stiffnesses are then prescribed given a known bounce frequency and the loads on each suspension cable. The next step consists of performing a nonlinear large displacement analysis with incremental loading and stiffness reformations at every step. The initial condition typically has the suspension springs unstretched with concentrated damping elements to damp the

system response. The iterations are performed until the structure reaches equilibrium under actual loading conditions. The end result of this step is a linear model of the statically deformed structure with geometric stiffening effects included. The third and final step is the eigensolution for infinitesimal displacements about the statically deformed configuration with the concentrated nodal damping elements removed.

Typical Results

Both 0-g and 1-g models were derived for the simple structure portrayed in Figure 3 with the primary payload rotated 45 degrees out of the vertical plane. The eigenfrequency shifts from the 0-g model to the 1-g model are shown in Figure 4. The rigid-body modes are all stiffened as they are replaced by bounce, tilt and pendular type modes while the flexible modes are variably stiffened and destiffened. Figure 5 shows two views of the modal cross-orthogonality mesh between the 0-g and 1-g eigenvectors. If the gravity effects were nil, the mesh would appear as a perfect diagonal due to orthogonality of modes. Clearly the rigid-body modes (low freq.) are perturbed the most resulting in a highly coupled subspace while flexible mode (high freq.) perturbations are largely limited to couplings between pairs of modes.

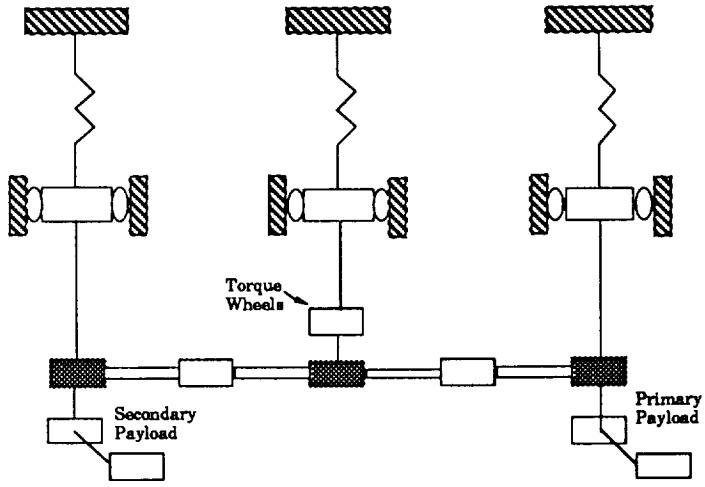

Figure 3. Simple analytical model for study of suspension and gravity effects.

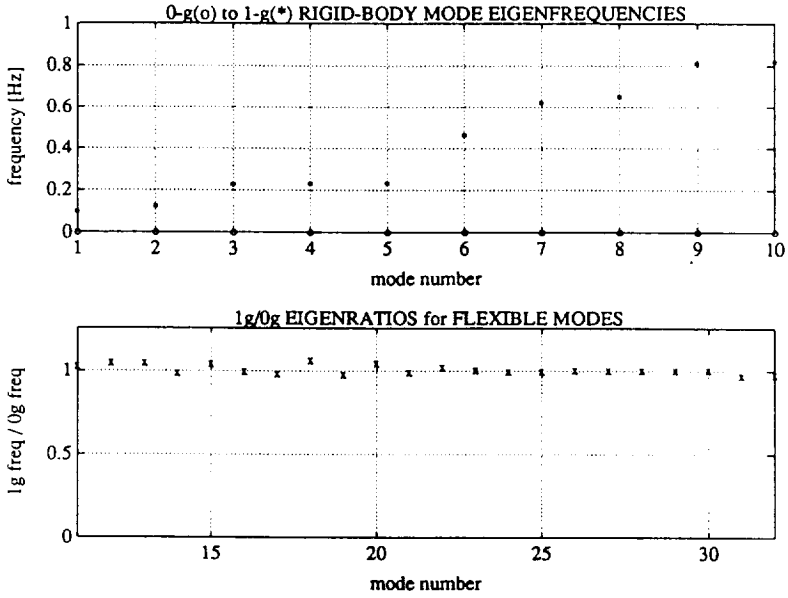

Figure 4. Eigenfrequencies for suspension modes and eigenratios for flexible modes.

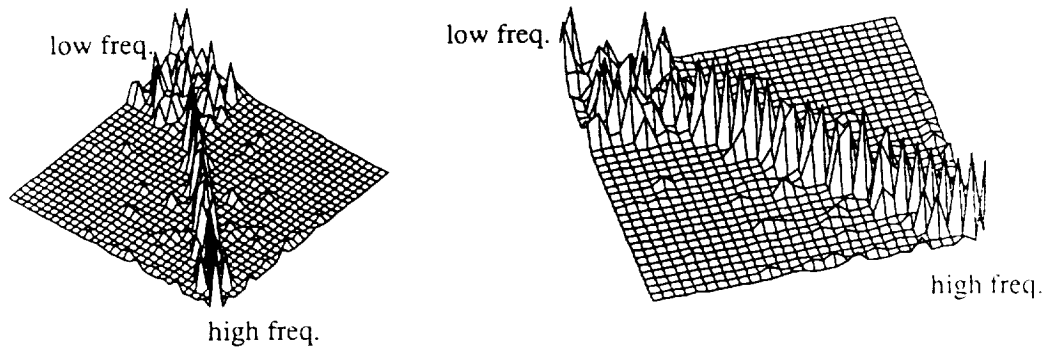

Figure 5. Modal cross-orthogonality mesh for 0-g and 1-g mode shapes.

Application to the MACE Development Model

An alternative means of visualizing the effects of suspension and gravity is to observe the perturbations to particular transfer functions through the structure. For this purpose, gravity effects were placed into a 0-g finite element model of the existing MACE DM hardware as shown in Figure 1. Figures 6a and 6b show the overlay of transfer functions from z-axis gimbal torque to the z-axis inertial angular rate of both the payload and the torque wheel assembly, respectively. The three transfer functions in each figure are from the 0-g model, 1-g model and measured data.

Notice at frequencies below 2 Hz that the 1-g model captures the payload pendulum and suspension

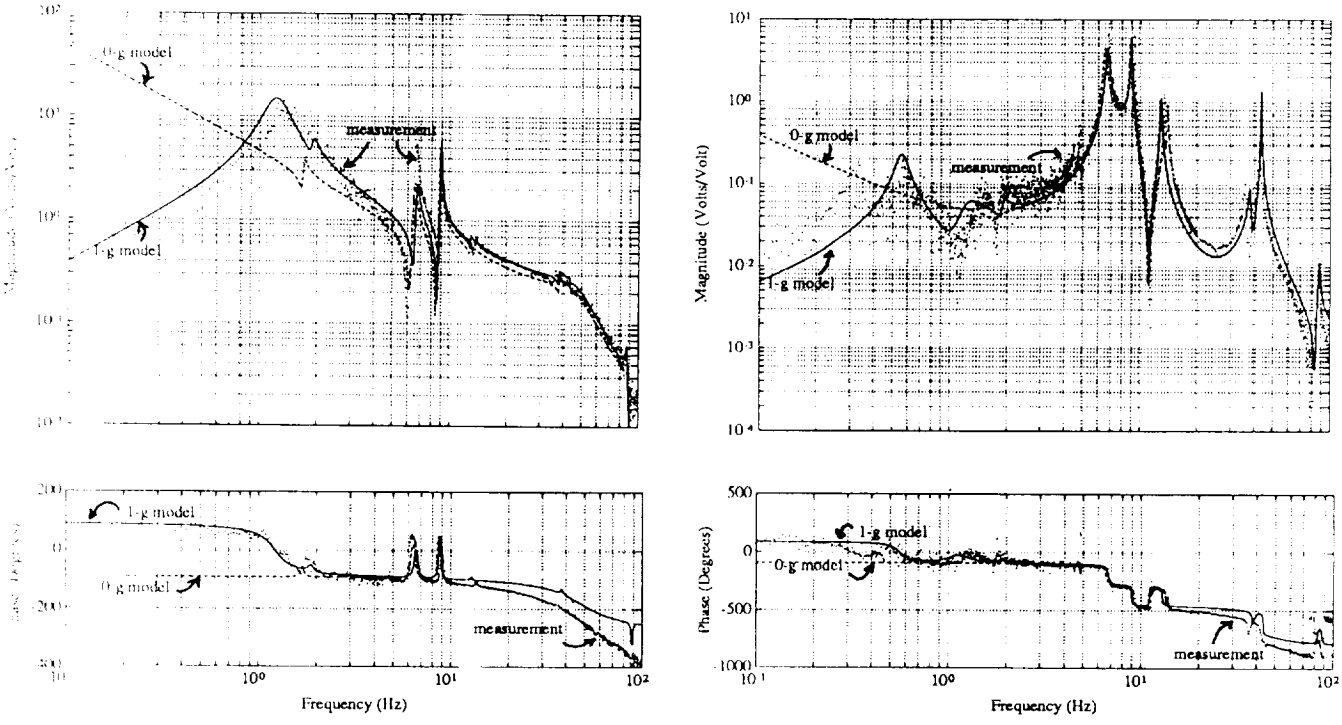

a) b)

Figure 6. Overlay of transfer functions from gimbal z-axis torque to a) payload z-axis inertial angular rate and b) bus inertial angular rate at the torque wheel location. Transfer functions are derived from measurements, the 1-g model and the 0-g model.

plunge modes while the 0-g model exhibits rigid body behavior. At higher frequencies, the 1-g model exhibits generally stiffer flexible modes than the 0-g model. This stiffening trend, caused by the gravity and suspension effects, appears to improve the agreement between the model and 1-g data as expected. Unmodelled time delays in the measurement devices could account for the deviation in modelled and measured phase behavior at higher frequencies.

Closed-Loop Control Analysis

With the 1-g and 0-g finite element models developed, one can now analyze the implications of testing the MACE test article in a 1-g environment when the control has been derived using a model of 0-g behavior. The model in Figure 3 was used for this analysis. For 0-g modelling, the suspension system is removed. The inertial angles of the primary payload and the inertial angles of the bus at the torque wheel location combine to form the performance metric. The gimbal motors in the secondary payload are used to generate torque disturbances on the structure. Both payloads are free to vary about their nominal positions.

The inputs to the plant are five torque actuators: three torque wheels for attitude control of the bus and two gimbal torque motors that rotate the primary payload about the relative x and z-axes. The physical outputs are taken to be 14 measurements: three inertial angles at the torque wheel assembly, two inertial angles at the primary payload, two relative gimbal angles, and the 7 corresponding angular velocities.

The 10 rigid body modes in the 0-g model are composed of three translations and three rotations of the bus, two rotations of the primary payload, and two rotations of the secondary payload. In the 1-g model, the presence of the suspension system results in no rigid body modes. All flexible modes are set to 1% damping. In the 1-g case, the 10 lowest frequency modes that correspond to pendulum-suspension modes are given 3% damping to account for the suspension system.

The presence of the 10 rigid body modes found in the 0-g structure are reflected in the complex frequency domain by the presence of 10 poles located at the origin. Thus, the rigid body modes are essentially pure integrators, which have infinite gain at DC. This presents a problem in the analysis in that any disturbance with low frequency content will be significantly amplified by the large low frequency gains of the rigid body modes. A two pronged approach is used to reduce the influence of the rigid body modes on the system. First, the performance of the closed-loop plant is evaluated using white noise bandlimited between 0.1 Hz and 60 Hz. This reduces the low frequency content of the disturbance. Second, the rigid body modes are stabilized using local proportional-differential (PD) feedback loops. The bus inertial angles and angular rates are fed to the torque wheels for rudimentary attitude control while the relative gimbal angles and angular rates are fed to the gimbal motors for coarse payload pointing.

The LQG controller design is carried out on the PD controlled 0-g model and then impinged on the 0-g and 1-g models. Behavioral differences are illustrated by plotting the performance versus increasing LQG control authority for both the 0-g and 1-g models. The intensity of the torque disturbance used to stimulate the PD controlled 0-g structure is adjusted to produce a 3σ performance (performance metric defined below) of 1 degree at low levels of LQG control authority. At high levels of control authority, it is desired that the LQG controlled 0-g system will exhibit a performance improvement of 40 db over the very low authority 0-g system. For the purposes of the design, the noise inputs are considered to be white. These assumptions avoid adding considerably more complexity to the design process and controller implementation. Although the assumption of white noise inputs will be made during the design process, the evaluation of the controller performance will take place using the closed-loop system with bandlimited noise.

The performance metric is chosen to be the weighted sum of the two payload inertial angles and the three bus inertial angles. This measure of performance emphasizes the inertial angular position of the primary payload while still recognizing that the inertial angular position of the bus must be bounded. The performance metric as a function of control authority for the total closed-loop system is shown in Figure 7a. Note that a new LQG design is performed for each level of control effort. The 0-g model shows a performance improvement of 36 db (40 db was the target) as the control authority is increased. For low control authority, the PD control stabilizes the rigid body modes of the 0-g system. The 1-g system has superior performance at low control authority due to the added damping and stiffness of the suspension system. However, as the control authority is increased on the 1-g system, its performance quickly deteriorates. An eigenvalue analysis indicates that a single closed-loop mode is driven unstable when the

control authority is increased. A participation factor analysis reveals that a suspension mode is the significant contributor to this instability.

Further evidence supporting this conclusion is obtained by subdividing both the 0-g and the 1-g models into flexible and nonflexible submodels. The closed-loop controller design procedure is then repeated. The submodel without any flexibility gives nearly identical performance to the model that included both flexible and nonflexible modes (Figure 7a). On the other hand, Figure 7b indicates that the performance of the flexible submodels for 0-g and 1-g begin to significantly distinguish themselves at a much higher level of control authority than the nonflexible submodels. This is an important result. In the 1-g environment, any potential instabilities of the flexible system that might occur at a high level of control authority are masked out by the deterioration in performance that occurs when the suspension modes are driven unstable at a relatively low level of control authority.

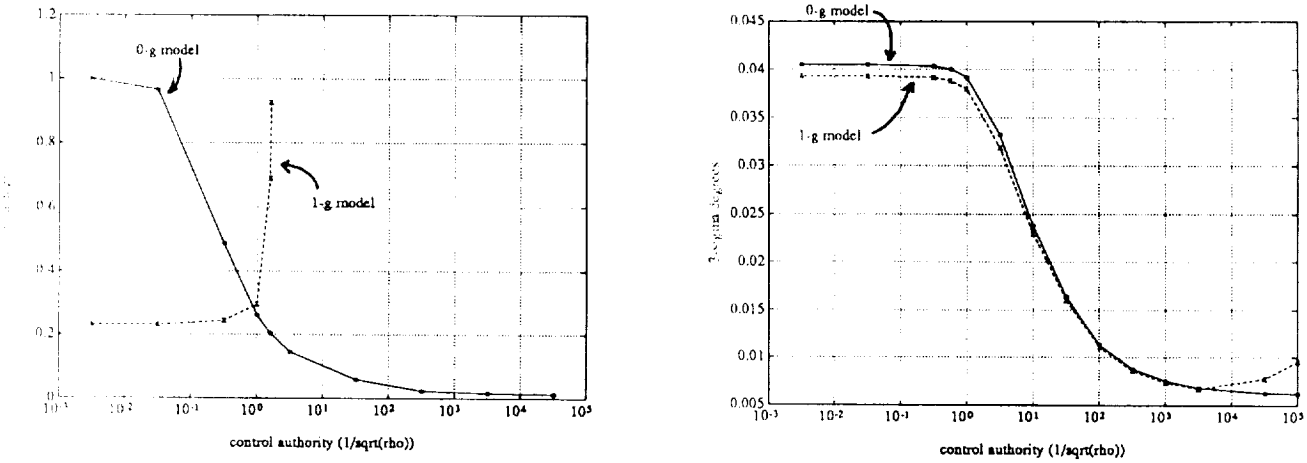

a) Total system b) Flexible modes only

Figure 7. Closed-loop performance versus control authority for controller designed with 0-g model and impinged on 0-g and 1-g models.

MEASUREMENT BASED CONTROL

Control Objectives

In parallel with the finite element analysis, experimental measurement based control was performed. The objective was to inertially point one axis of the payload while a band-limited white noise disturbance was introduced through the gimbal torque motor. The control problem was posed to primarily involve control of flexible response in the x-y plane as shown in Figure 8. Therefore, all measured angles and actuated torques in the experiments were about the z-axis. Two different feedback architectures were used.

In the first architecture, the inertial angle of the payload was fed through a dynamic feedback compensator to drive the gimbal motor (Figure 8a). This resulted in a control problem where both the feedback sensor (**y**) and performance metric (**z**) were the inertial angle of the payload and the disturbance (**w**) and control signals (**u**) both entered the structure through the gimbal motor. This is referred to as the single-input, single-output (**SISO**) control problem.

In the second architecture, the feedback sensors were the the inertial angle of the torque wheels (**y**) and the relative gimbal angle as measured by the optical encoder (**y**) (Figure 8b). Along with a model of the intervening flexibility, the control formulation could employ the inertial bus and relative gimbal angles to make the inertial angle of the payload observable. Again, the gimbal torque motor acted as both the disturbance source (**w**) and control actuator (**u**). This resulted in a single-input, two-output (**SITO**) feedback architecture. A SITO controller was first formulated for the performance metric discussed above (**z** in Figure 8b). Then this metric was augmented by the addition of the bus inertial angle (**z** in Fig. 8c). This combined metric forced the control to attenuate flexible motion of the bus in addition to isolating the payload.

In total, three sets of experiments were conducted: **1)** SISO control to minimize payload pointing

error; 2) SITO control to minimize payload pointing error; and 3) SITO control to minimize a combination of payload pointing error and bus attitude. For each experiment, measurements of the pertinent transfer functions through the hardware were used to formulate a measurement model. The pertinent transfer functions were from the disturbances and actuators to both the feedback sensors and performance metric. These functions were fitted using poles, zeros, a gain and a time delay. Once the poles and residues of these transfer functions were placed in state-space form, Linear Quadratic Gaussian (LQG) control was derived. While the resulting dynamic compensators were implemented on an AC-100 real time control computer, the transfer functions from the disturbance to the performance metric were measured. These measurements were finally used to evaluate performance. The following two sub-sections present the evolution from modelling to closed-loop results for the SISO and SITO control architectures.

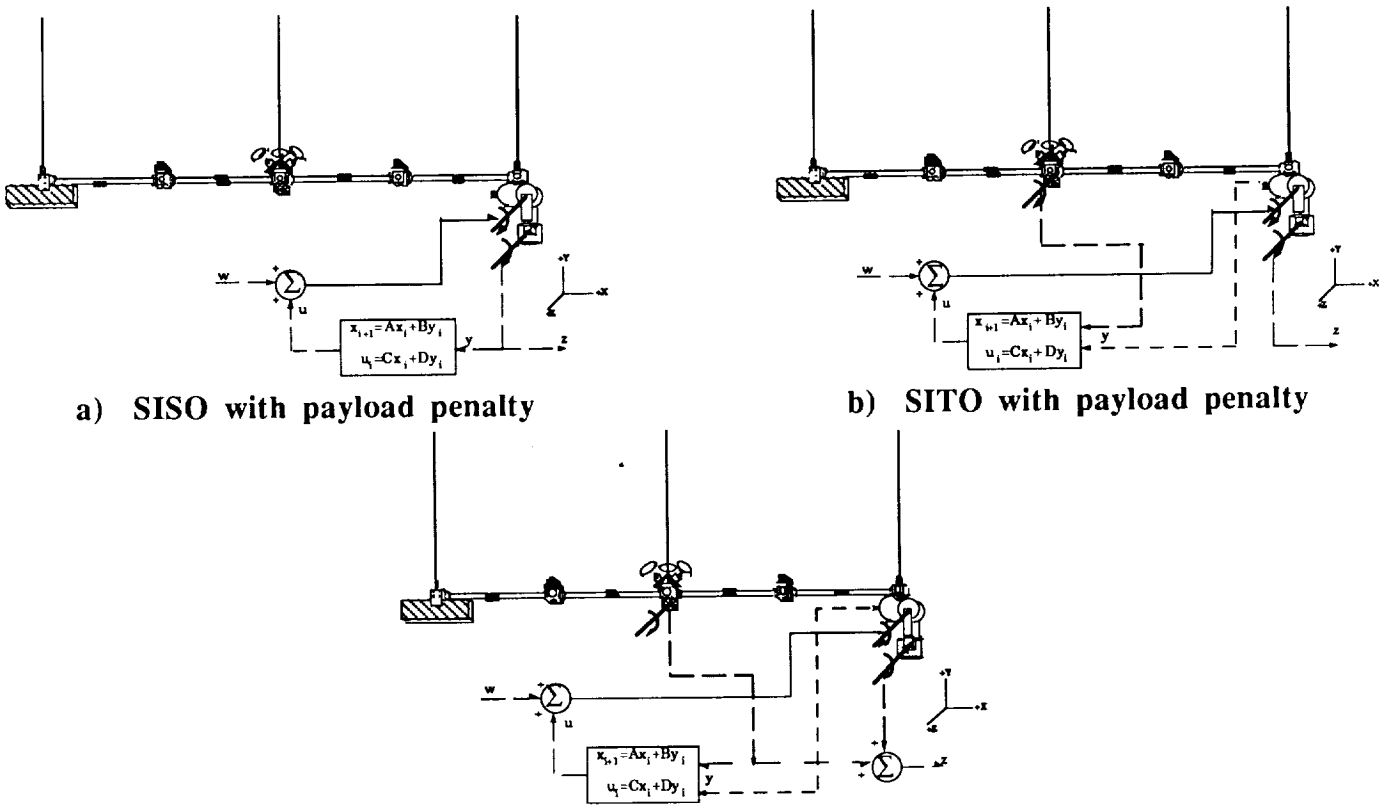

a) SISO with payload penalty

b) SITO with payload penalty

c) SITO with payload and bus penalty

Figure 8. Disturbance, performance metric and feedback architectures for the experiments.

Single-Input, Single-Output Control Architecture

A measurement model of the DM was obtained by measuring the transfer function from the gimbal torque to the payload inertial angle. This SISO transfer function was fit using poles, zeros, a static gain and a time delay which were then placed into continuous state-space form. Figure 9a overlays the measured transfer function (Data) with that calculated using the fitted parameters (Fit). The two resonances between one and two Hertz represent the pendulum mode of the gimbal and the first bending mode of the bus. Additional flexible modes occur near 7 and 9 Hz. The model contained 10 structural states and a third order Pade approximation to the time delay to yield a 13 state control design model.

Figure 9b overlays the open-loop (OL) and several closed-loop transfer functions from the gimbal disturbance to the inertial angle of the payload. The prediction of the closed-loop transfer function and the actual measurement were in very close agreement. This was made possible by the accuracy of the nonlinear fit. At low levels of control authority, the control reduced the static, pendulum and first bending mode

responses (CL1). The plant inverting dynamics in the compensator left the higher frequency modes almost unaffected. As authority was increased, the second bending mode near 7 Hz started to be suppressed. Eventually, all of the flexible dynamics visible in Figure 9b were suppressed (CL2). The closed-loop improvement in the RMS inertial payload angle was over one order of magnitude.

The same compensators were implemented several weeks later. A shift in the frequencies of the modes near 9 Hz caused instability when the compensator corresponding to CL2 was implemented. The highest level of control authority that was stable at this later date corresponds to CL1. Since the compensator performs plant inversion of the 9 Hz dynamics, stability is highly sensitive to slight shifts in these dynamics over time. To reduce this sensitivity, a multimodel technique (ref. 16) was used to derive the control. Control was designed to yield a given level of performance when applied to either model. The two chosen models differed by slight shifts in the frequencies of the dynamics near 9 Hz. The closed-loop response (CL3 in Figure 9b) using this new compensator was stable and exhibited adequate gain and phase margin despite the fact that the two models were based upon several week old data.

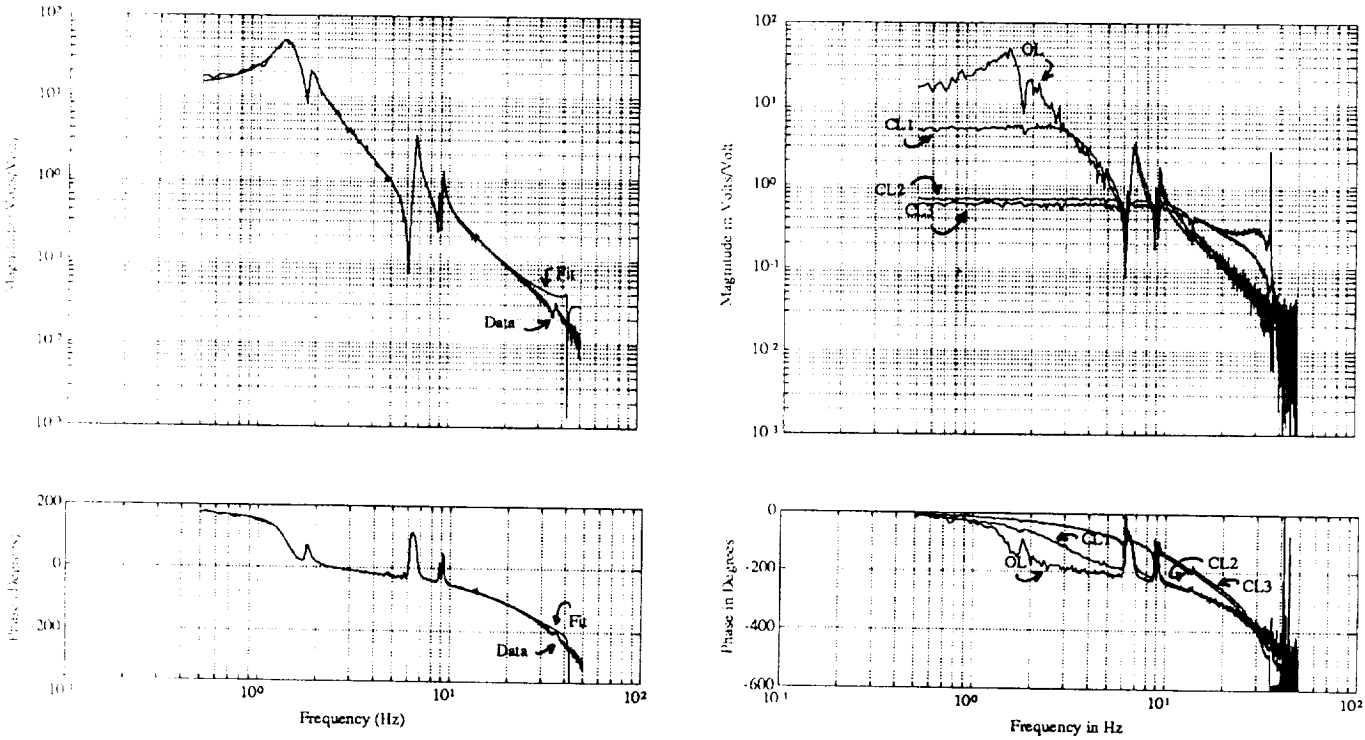

a) b)

Figure 9. a) **Data and pole-zero fit to the transfer function from z-axis gimbal torque to payload inertial angle.**

b) **Measured open and closed-loop transfer functions from gimbal disturbance to payload inertial angle.**

Single-Input, Two-Output Control Architecture

Three transfer functions were measured for this model. The first transfer function is shown in Figure 9a and represents the transfer function from both the disturbance and control actuator (gimbal) to the performance metric (payload inertial angle). The second transfer function was from gimbal torque command to relative gimbal angle as measured by an optical encoder (Figure 10a). The third transfer function was from gimbal torque to the bus inertial angle (Figure 10b). These last two measurements corresponded to the

transfer functions from the actuator to the feedback sensors.

The next step in the model development used a nonlinear fit routine to fit left half plane complex pairs of poles and zeros along with gains and time delays to these three transfer functions. Nonminimum phase zeros were required to achieve the fit to the noncolocated transfer function shown in Fig. 10b (Fit). The next step involved placing the poles, zeros, gains and time delays into state-space form.

Figure 11 overlays the open and highest authority closed-loop transfer functions from the gimbal disturbance to the payload inertial angle for SITO control with payload penalty (Fig. 8b). As in the SISO results, the control first reduced the 1.0 to 2.0 Hz response composed of the payload pendulum and first bending modes and then started to reduce second bending near 7 Hz. At low levels of control authority, the modes near 9 Hz were destabilized due to inaccuracies in the plant inversion being attempted by the compensator. To correct this, a lead compensator was added by placing a lightly damped pair of zeros just below the two modes near 9 Hz followed by a lightly damped pair of poles just above these modes. The increase in gain and phase margin allowed the control authority to be increased to the level which was used to obtain the result shown in Fig. 11.

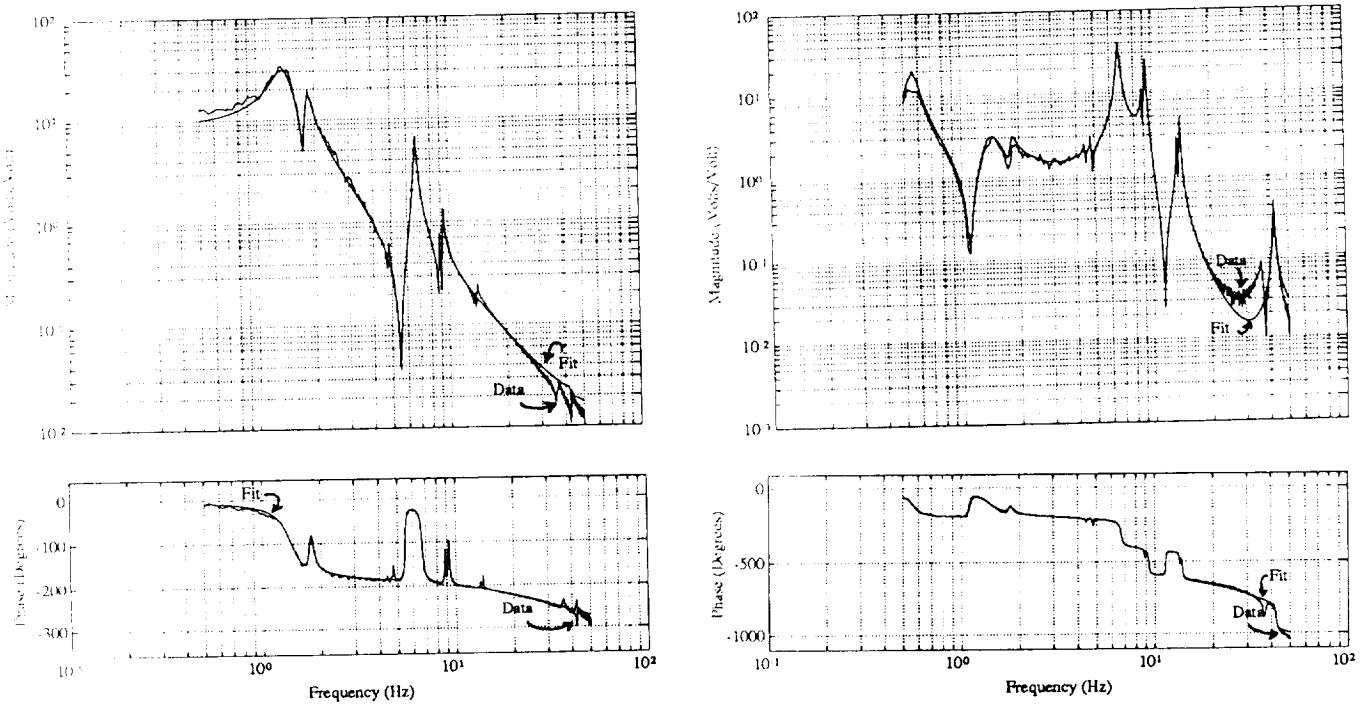

Figure 10. Data and pole-zero fit to the transfer function from z-axis gimbal torque to a) encoder angle and b) bus inertial angle.

As might be expected by observing Figures 10b, the addition of bus angle to the performance metric will cause the control to concentrate more on reducing flexible motion. The control will not only focus on reducing the payload pendulum and first bending modes, which dominate response in Fig. 9a, but to also suppress the flexible modes at 7 and 9 Hz, which dominate the response in Fig. 10b. As expected, the payload pendulum and first bending modes observed in the gimbal to payload inertial angle transfer function were suppressed (Figure 12a). Figures 12a and 12b show that the flexible modes near 7 and 9 Hz were also suppressed. In fact, the response in this frequency regime is reduced by an order of magnitude more than the level in Figures 9b and 11. Notice that the response is increased at frequencies above 10 Hz as a sacrifice for the dramatic reduction at low frequencies. In general, all of the closed-loop ground experiments achieved over an order of magnitude reduction in payload pointing error.

FLIGHT EXPERIMENT

The on-orbit science operations are designed to compliment the ground test program as shown in Figure 2. The on-orbit experiment exploits the unique shirt sleeve environment of the Shuttle middeck. Figure 13 shows the test article in the Shuttle middeck. The basic hardware and operations will mimic that of the Middeck 0-Gravity Dynamics Experiment (MODE) which flew on Discovery during the STS-48 mission in September, 1991 (ref. 13). In total, the MACE experiment will require three 8-hour days of one crew member. The assistance of a second crew member will be necessary periodically. The test article, data storage disks, and other support equipment will be stored in a disassembled fashion in three middeck lockers. A fourth locker will contain the Experiment Support Module (ESM). This package contains the experiment control computer, the real time control computer, data acquisition and storage, signal conditioning and power amplification electronics. A hand held keypad and display will enable the crew member to control the experiment and a digital interface to a portable computer will give access data analysis software and STS downlink channels.

The first on-orbit experiment in the summer of 1994 will involve open-loop system identification. Time response data will be measured from the disturbance source and control actuators to the feedback sensors and performance metric and stored in the ESM. Depending upon the final form of downlink available, either time or frequency domain data will be downlinked to the ground. This data will first be used to possibly restructure the sequence of pre-programmed control protocols. In addition, a measurement model will be developed for use in formulating 0-g measurement based control. Additional open-loop identifications will be conducted at the beginning of every science operations day.

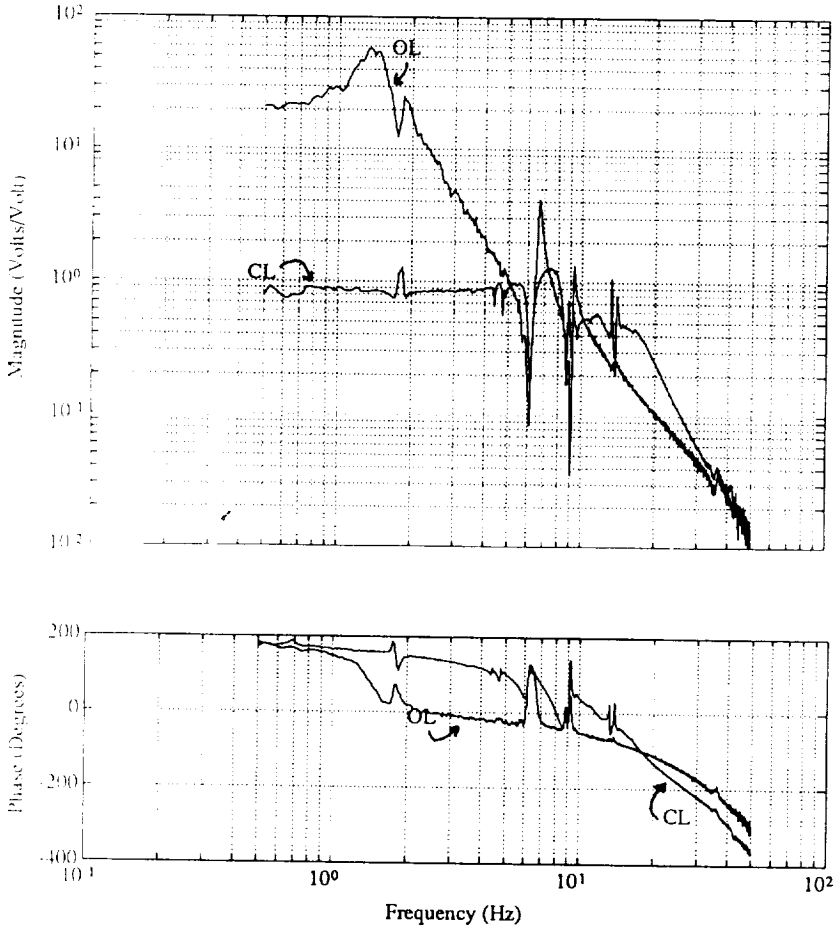

Figure 11. Measured open and closed-loop transfer functions from disturbance to payload angle for SITO control with payload penalty.

The on-orbit closed-loop tests will involve two classes of controllers. The first class will be derived using the analytical predictions of 0-g behavior. The finite element model, which will have undergone refinement through ground testing and analysis, will have the gravity effects removed. This 0-g model will then be used to formulate controllers. The on-orbit performance of these controllers, at various levels of control authority, will be compared to finite element predictions. As the 0-g results and 1-g predictions diverge, a feel for predictive accuracy achieved through analysis and ground testing will be obtained.

The second class will use system identification data, downlinked from the Orbiter, to develop a measurement model. The resulting controllers will be uplinked several days later for implementation. This class of controller investigates the performance improvements that are achievable through on-orbit identification and control reconfiguration.

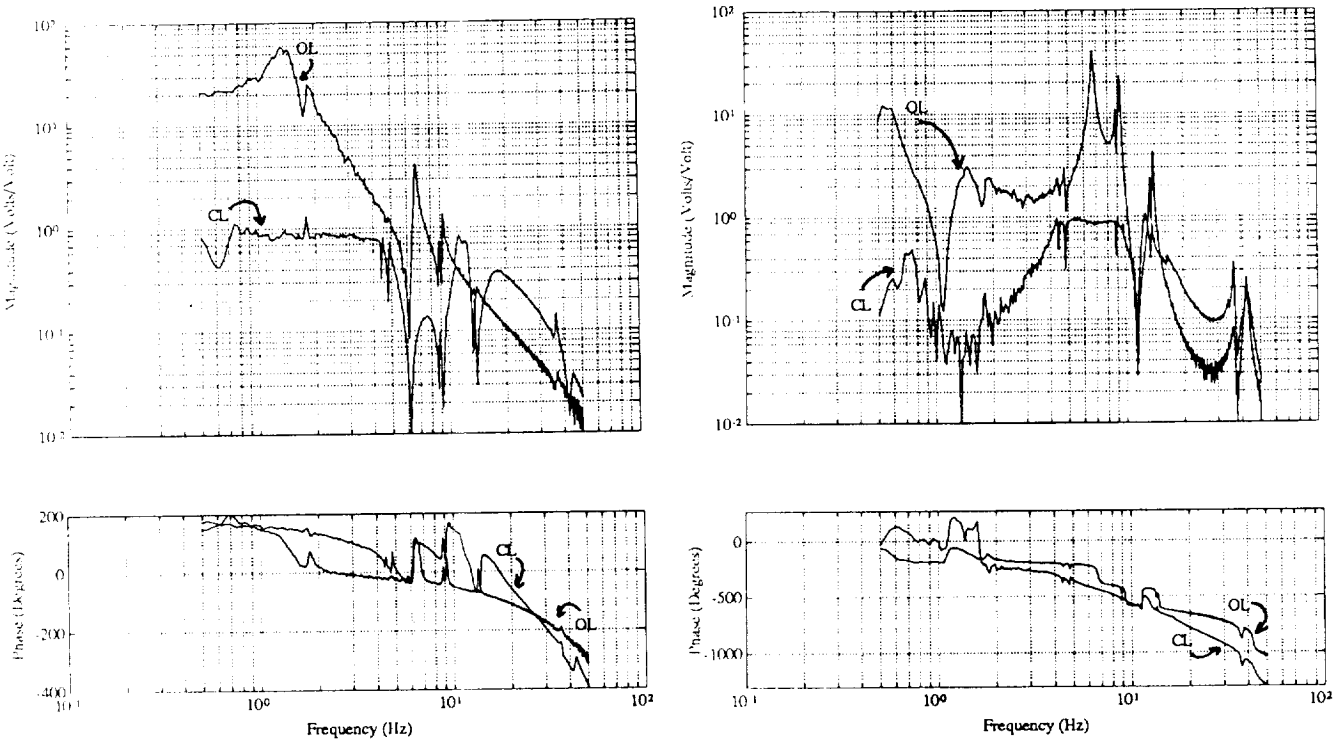

Figure 12. Measured open and closed-loop transfer functions from disturbance to a) payload angle and b) bus inertial angle for SITO control with payload and bus penalty.

SUMMARY

The Middeck Active Control Experiment (MACE) is designed to study the ability to predict and tune on-orbit control performance given analysis, ground testing, and 0-g system identification. The science approach for MACE exploits both analytical and measurement models to generate predictions of on-orbit performance.

Analytical models developed using finite element analysis incorporate suspension effects, stiffness effects and static pre-deformations. The use of these effects improves the agreement between model predictions and ground test data. Further refinement is achieved through open and closed-loop ground testing of the hardware. The gravity and suspension effects are removed from the analytical model for the formulation of controllers for tests on orbit.

Analytical modelling of the MACE test article showed that a low fundamental frequency, multiple payload device exhibits significant suspension and gravity coupling. Linear Quadratic Gaussian controllers designed for on-orbit operation, but subjected to these effects on the ground, were shown capable of first

destabilizing suspension modes and then flexible modes at higher levels of control authority. This makes ground testing of candidate on-orbit controllers difficult. Therefore, the accuracy of on-orbit predictions would be unknown. In order to improve on-orbit performance limited by prediction error, 0-g system identification data will be used to develop a measurement model for tuning the control on orbit.

Measurement models have been developed and Linear Quadratic Gaussian controllers have been implemented in the laboratory. In general, Linear Quadratic Gaussian control proved to be very effective at achieving significant performance improvements under broadband disturbance. Over an order of magnitude reduction in pointing error was achieved. However, the plant inversion that LQG employs cannot tolerate changes in test article dynamics. Both multimodel and classical design techniques were used to make the control more robust.

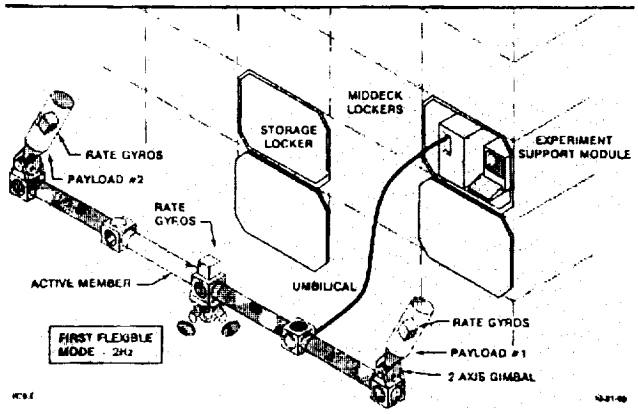

Figure 13. Test article deployed on the middeck.

ACKNOWLEDGEMENTS

This work is supported by the NASA In-Step and CSI Offices with Mr. Anthony Fontana as technical monitor. Special thanks to Mr. Douglas MacMartin and Mr. Jonathan How for their invaluable assistance in the control design.

REFERENCES

1. Experiment Requirements Document, MACE Document No. MACE-1-101, M.I.T. Space Engineering Research Center, Oct. 1991.
2. Miller, D. W.; de Luis, J.; Crawley, E. F.: Dynamics and Control of Multipayload Platforms: The Middeck Active Control Experiment (MACE). Proceedings of the 41st International Astronautical Federation Congress, Dresden, GDR, paper No. IAF-90-292, Vol. 24 of Acta Astronautica, Oct 6-12, 1990.
3. Wada, B. K.: Adaptive Structures. 89-1160-CP, presented at the 30th Structures, Structural Dynamics and Materials Conference, Part 1, Mobile, AL, 1989, pp. 1-11.
4. Chen, J-C; Fanson, J. L.: System Identification Test Using Active Members. AIAA 89-1290, presented at the 30th Structures, Structural Dynamics and Materials Conference, Mobile, AL, April, 1989, pp. 1154-1163.
5. Gilpin, K.; Athans, M.; Bokor, J.: Identification of a Lightly Damped Structure for Control-Structure Interaction. M.I.T. SERC #11-91, August, 1991.
6. Sidman, M. D.; DeAngelis, F. E.; Verghese, G. C.: Parametric System Identification on Logarithmic Frequency Response Data. IEEE Transactions on Automatic Control, Vol. 36, No. 9, September, 1991, pp. 1065-1070.

7. Crawley, E. F.; de Luis, J.; Miller, D. W.: Middeck Active Control Experiment: Phase A Final Report. MIT-SSL Report #7-89, 1989.
8. Rey, D. A.; Crawley, E. F.; Alexander, H.: The Direct Effects of Gravity on the Control and Output Matrices of Controlled Structure Models. AIAA 92-2094, presented at the AIAA Dynamics Specialist Conference, Dallas, TX, April 1992.
9. Kienholz, D. A.: A Pneumatic/Electric Suspension System for Simulating On-Orbit Conditions. 90-WA/Aero-8, presented at the Winter Annual Meeting of the American Society of Mechanical Engineers, Dallas, TX, November, 1990.
10. Using the AC-100: AC-100 User's Guide v2.4.03A. Integrated Systems Inc., November, 1990.
11. Kwakernaak, H.; Sivan, R.: *Linear Optimal Control Systems*. Wiley-Interscience, John Wiley & Sons, Inc., 1972.
12. Rey, D.A.: The Direct Effects of Gravity on the Control and Output Matrices of Controlled Structure Models. AIAA Paper No. 92-2094, 33rd AIAA Dynamics Specialist Conference, Dallas, April 1992.
13. Crawley, E. F.; Miller, D. W.; van Schoor, M.; de Luis, J.: Middeck 0-Gravity Dynamics Experiment: Project Plan. MIT-SSL Report 9-89, 1989.
14. ADINA User's Manual. ADINA R&D, Watertown, MA, 1987.
15. Crawley, E.F.; Barlow, M.S.; vanSchoor, M.C.; Bicos, A.: Variation in the Modal Parameters of Space Structures. Presented at the 33rd Structural Dynamics and Materials Conference, Dallas, April 1992.
16. MacMartin, D. G.; Hall, S. R.; Bernstein, D. S.: Fixed-Order Multi-Model Estimation and Control. Presented at the 1991 American Control Conference, Boston, MA.

SESSION V

Chairman: Brantley R. Hanks
NASA Langley Research Center
Hampton, Virginia

Co-Chairman: Capt. Chuck Sherwin
Phillips Laboratory
Edwards AFB, California